Indian journal of
Engineering

To Cite:
Vijayan A, Ashok S. Numerical analysis of a visual servo system with Relative Gain Array. *Indian Journal of Engineering*, 2023, 20, e36ije1672 doi: https://doi.org/10.54905/disssi.v20i54.e36ije1672

Author Affiliation:
Department of Electrical Engineering, Government Engineering College, Painavu, Idukki, Kerala, India

*Corresponding Author
Department of Electrical Engineering, Government Engineering College, Painavu, Idukki, Kerala,
India
Email: abhilash@gecidukki.ac.in

Peer-Review History
Received: 14 October 2023
Reviewed & Revised: 18/October/2023 to 18/December/2023
Accepted: 21 December 2023
Published: 29 December 2023

Peer-Review Model
External peer-review was done through double-blind method.

Indian Journal of Engineering
pISSN 2319–7757; eISSN 2319–7765

DISCOVERY
SCIENTIFIC SOCIETY

Numerical analysis of a visual servo system with Relative Gain Array

Abhilash Vijayan*, Ashok S

ABSTRACT

The generation and characterization of control signals for decision-making in industrial robotic applications require essential data from the environment, gathered through various sensors. Atop these sensors, a camera is employed to collect information and data from the surroundings. Visual feedback proves to be an effective and robust technique for closed-loop robotic applications. This paper proposes a multivariable interaction model, akin to process control, for the visual-servo system. Variable interaction is inherent in these Multiple Input Multiple Output (MIMO) system models, which is apt for explaining the intrinsic flaws of Image-Based Visual Servoing (IBVS). Singular Value Analysis (SVA) and Relative Gain Array (RGA) serve as pragmatic tools for the evaluation and analysis of the system. The objective of this paper is to utilize RGA for the numerical analysis of the visual servo control structure.

Keywords: Visual servoing, MIMO, Condition Number, RGA, SVA

1. INTRODUCTION

Feedback control in robotics involves the collection of relevant sensor data from the environment to generate control signals for guiding robot movements for achieving specific goals. Visual data obtained from sensors serves as input for the control system, facilitating the derivation of signals for guidance, supervision, and feedback control. In automated industrial settings, robots play pivotal roles in tasks such as cutting, picking, placing, welding, and sorting. Vision sensors due to their non-contact nature enhance the performance of these systems. The substantial amount of data captured by cameras regarding the robot's surroundings also enables the implementation of heuristic approaches in control. With the advancements in sensor technologies, efficient image processing techniques, and high-speed processors, visual servoing has become an integral component of closed-loop feedback control systems for robots. This paper aims to conceptualize visual feedback control as a multivariable control system and assess its properties using Relative Gain Array (RGA).

Visual servoing employs sensors such as cameras to generate feedback signals for a robot. Sensory information, obtained as perceptible features from the image, provides details about the pose of both the robot and the target. This information is processed by the servo-controller to generate velocity

screws. With a comprehensive understanding of the workspace geometry and its transformational relationships, the controller directs the robot's motion. Visual-servo systems are categorized as either Image-Based Visual Servoing (IBVS) or Position-Based Visual Servoing (PBVS). In IBVS, the error signal is directly derived from the image features, ultimately mapping to signals for the robot's motion. This scheme explicitly governs the trajectory, ensuring that the target remains within the camera's view. IBVS exhibits no computational delay compared to PBVS, where features extracted from the image and models of the camera and workspace are required to estimate the target pose.

PBVS is recognized for offering manipulator trajectories feasible in a global sense, but there is a risk of the tracked object moving out of the camera's view. A comprehensive study and explanation of coordinate transformations, essential classes, structures, and the taxonomy of visual servo systems can be found in previous works (Chaumette and Hutchinson, 2006; Siebel et al., 2010). IBVS and PBVS exhibit inherent shortcomings during servoing. In IBVS, the estimation of depth is essential, and an inadequate evaluation of depth can lead to system instability. Inaccurate depth estimations can result in disorderly trajectories for the manipulator as it navigates to its destination, affecting the final pose and introducing errors. On the other hand, for PBVS, accurate estimation of 3D parameters is crucial, as they contribute to the computation of the error. Coarse estimations may lead to inaccuracies in the final pose and perturbations in the trajectory.

In theory, the Cartesian space trajectory is considered optimal, but this may not be true in the image plane. Even small errors in image measurements can result in significant pose errors, affecting the overall accuracy of the system. However, the 2D vision sensor in IBVS demonstrates resilience to calibration errors and noise. For distant targets, initial camera motions can be substantial without appropriate gain, and there is a risk of encountering local minima or singularities in the image Jacobian. Specific configurations may lack optimal paths, leading to unpredictable camera motion. IBVS offers bounded stability, while PBVS provides global stability (Hutchinson et al., 1996; Deguchi, 1998). To address the limitations of basic schemes, there are various hybrid, switched, or partitioned schemes in visual servoing designed to combine advantages or mitigate drawbacks (Hutchinson et al., 1996; Deguchi, 1998).

The complexity of the visual feedback structure escalates with an increase in degrees of freedom (DoF). In the case of a robot with 6-DoF requiring displacement, each joint may need to move accordingly. In visual servo systems, one joint typically controls one degree of freedom. Velocity control signals at the joint level can govern joint motion, representing it as a linearized model Gangloff and de-Mathelin, (2000) in an open loop with multiple inputs and outputs. Process control and industrial applications commonly involve multiple variables in both input and output, resulting in a multi-variable structure. The manipulated variables serve as the input, influencing the values of the output variables. Cross-linkages between controlled and manipulated variables are possible. Control in Multiple Input Multiple Output (MIMO) systems is inherently more intricate than in Single Input Single Output (SISO) systems (Seborg, 2011). Addressing MIMO problems necessitates determining the most appropriate pairing between controlled and manipulated variables.

Singular Value Analysis (SVA) and Relative Gain Array (RGA) Bristol, (1966) prove useful for analyzing such systems. Through SVA, the Condition Number (CN) can be computed as the ratio of the peak and bottom values of nonzero singular values, serving as an indicator of the system's performance. SVA also provides an assessment of the robustness of the control structure. Effective handling of these systems involves strategies such as the separation of interacting variables and the application of other multi-variable control techniques. RGA offers a method to quantify variable interaction, suggesting suitable variable pairings for improved control. Significant Relative Gain Array (RGA) elements indicate robustness challenges in the process control industry. The Condition Number also highlights difficulties in finding a solution to the control problem, with the mapping between input and output variables influencing the Condition Number.

In instances of deviations, larger values of RGA elements signal deviations (Chen et al., 1994). Robot manipulability and Condition Number are sometimes used as performance indices in parallel robots (Merlet, 2006). Specific feature points can lead to the singularity of the interaction matrix, and the inverse of the Condition Number aids in analyzing such singularities. In the case of diagonal controllers, RGA can determine suitable input-output pairings, aligning with the principles of decoupling in control. The use of RGA as a tool for analyzing performance characteristics is discussed in (Vijayan and Ashok, 2017). This paper will introduce a visual feedback scheme as a Multiple Input Multiple Output (MIMO) system and utilize RGA to analyze the system behavior through numerical examples. Subsequent sections will elaborate on the model of the visual feedback system, the multivariable model, numerical analysis using RGA, and the presentation of results and conclusions.

2. VISUAL SERVO SYSTEM

The objective of visual servoing is to drive the robotic manipulator from its current position to the desired point with the help of a camera. The control structure will try to minimize an error e between present image features $s(t)$ and s^*. The former set comprises a vector of k visual features extracted from the camera view along with additional information like camera intrinsic parameters. In contrast, the latter set includes the desired value of features.

$$e(t) = s(t) - s^* \quad (1)$$

The selection of image features is important and influences the nature of the control law. Point features, line features, and any other key points with perceivable traits or measurable attributes from pixel data like centroid, and moment calculation may constitute the visual features.

Consider a feature located at $P(X,Y,Z)$ in the world point transformed as $p(x,y)$ in the image plane with the transformation, $x = x/z$ and $y = y/z$. In terms of pixel coordinates, the relation $p\,(u,v) = f(P,K,{}^{c}_{t}T)$ holds the information regarding K, the camera matrix ${}^{c}_{t}T$, the target pose with respect to the camera, f, the focal length and (c_u, c_v) the principal point. The variation of $p(x,y)$ in time is given by

$$\dot{p} = J_s(p)v \quad (2)$$

J_s is the image Jacobian and $v = (\vartheta_c, \omega_c)$ is the velocity of the camera with respect to the target. $\vartheta_c = [\vartheta_x, \vartheta_y, \vartheta_z]$ and $\omega_c = [\omega_x, \omega_y, \omega_z]$ represent the linear and the angular velocity of the camera respectively. The variation of the image point $p(x,y)$ in time is

$$\begin{bmatrix}\dot{x}\\ \dot{y}\end{bmatrix} = \frac{1}{Z^2}\begin{bmatrix}\dot{X} - XZ\dot{Z}\\ \dot{Y} - YZ\dot{Z}\end{bmatrix} \quad (3)$$

The change in world point view with respect to camera will be

$$\dot{P}(X,Y,Z) = -\vartheta_c - \omega_c \times P(X,Y,Z) \quad (4)$$

Expanding the change in the 3D point, $\dot{P}(X,Y,Z)$ along X, Y and Z axes, the components are

$$\left.\begin{aligned}\dot{X} &= Y\omega_z - Z\omega_y - \vartheta_x\\ \dot{Y} &= Z\omega_x - X\omega_z - \vartheta_y\\ \dot{Z} &= X\omega_y - Y\omega_x - \vartheta_z\end{aligned}\right\} \quad (5)$$

Combining the (3) and (5)

$$\begin{bmatrix}\dot{x}\\ \dot{y}\end{bmatrix} = \begin{bmatrix}-\frac{\vartheta_x}{z} + \frac{x\vartheta_z}{z} + xy\omega_x - (1+x^2)\omega_y + y\omega_z\\ -\frac{\vartheta_y}{z} + \frac{y\vartheta_z}{z} + (1+y^2)\omega_x - xy\omega_y - x\omega_z\end{bmatrix}$$

$$= \begin{bmatrix}-\frac{1}{z} & 0 & \frac{x}{z} & xy & -(1+x^2) & y\\ 0 & -\frac{1}{z} & \frac{y}{z} & 1+y^2 & -xy & -x\end{bmatrix}\begin{bmatrix}\vartheta_x\\ \vartheta_y\\ \vartheta_z\\ \omega_x\\ \omega_y\\ \omega_z\end{bmatrix} \quad (6)$$

This equation is of the form, $\dot{p}(x,y) = J_{p(x,y)}V_c$

$J_{p(x,y)} = \begin{bmatrix}-\frac{1}{z} & 0 & \frac{x}{z} & xy & -(1+x^2) & y\\ 0 & -\frac{1}{z} & \frac{y}{z} & 1+y^2 & -xy & -x\end{bmatrix}$ is the interaction matrix having $n \times k$ elements and where n represents the degrees of freedom and k the image coordinates selected. The above matrix holds the Jacobian values for a single point. As the features increase, the values are stacked to form the whole Jacobian. Selecting the feature coordinates as the image feature of interest, $e_p = s_{p(x,y)} - s^*$. The error changes exponentially with the choice of a control gain λ.

$$\dot{e}_p = -\lambda e_p \quad (7)$$

For an eye-in-hand system, the end effector carries the camera. Hence, end effector velocity and camera velocity V_c are the same.

$$V_c = -\lambda {J_p}^{+} e_p \quad (8)$$

When the robot DOF is less than or not equal to the number of image points selected, the interaction matrix is not invertible and hence ${J_p}^{+}$ is the Moore-Penrose pseudoinverse. Matrix is invertible when n and k are equal.

The uncertainties and disturbances within the system can give rise to different types of noise. Various noise models are utilized to address and mitigate these sources of noise within the system. Noise may manifest in different aspects, including image measurement, pose measurement, feature extraction, or due to system dynamics and environmental factors. In this study, image

noise is accounted for during camera calibration, while uncertainties are modelled within the process control model. The experimental setup comprises an ABB IRB 1200 robot with a Webcam (LogiTech C-270, 8MP) attached to its end effector. A pneumatic gripper, programmable through the Flexpendant, serves as the tool for closing and opening. Visual feedback is obtained through the end effector camera, capturing images during the operation. The target itself is a rectangular block featuring distinguishable point features. The target's bounding box edges provide essential features for the control law.

Techniques such as template matching or feature extraction can be employed for target identification. Speeded Up Robust Features (SURF) are utilized due to their ability to extract information from cluttered scenes. Reference values are either pre-known or can be determined by projecting the image onto a plane parallel to the camera front, especially when the target's shape is available. The gripper's closing height establishes the reference values. The error is then calculated by comparing the current image feature values with the corresponding reference values. Utilizing the control law outlined in equation (8), the incremental change in pose necessary to guide the end effector towards the target is computed. The flow of control signals is illustrated in the accompanying figure. The robot's pose is determined from the Flexpendant values. The robot's movement can be accomplished in two manners: either by computing the new pose based on the current value and the incremental change or by directly applying the latter.

To ensure that the newly assigned pose consistently falls within the robot's reachable workspace, the former method is employed in this context. The calculation of the new pose to which the robot must move is performed and communicated to the controller. This process is reiterated until the system satisfies the criterion regarding the error norm. For the implementation of Image-Based Visual Servoing (IBVS), a target is maintained within the field of view of the eye-in-hand camera. Utilizing Speeded Up Robust Features (SURF), the object is identified. The four corners of the rectangular box housing the target are identified as features for visual servoing. Desired features are pre-determined by keeping the gripper at a height from which the target can be grasped. Figure 1 illustrates the variation in components of the end effector camera pose from an initial position where the target is visible to the camera.

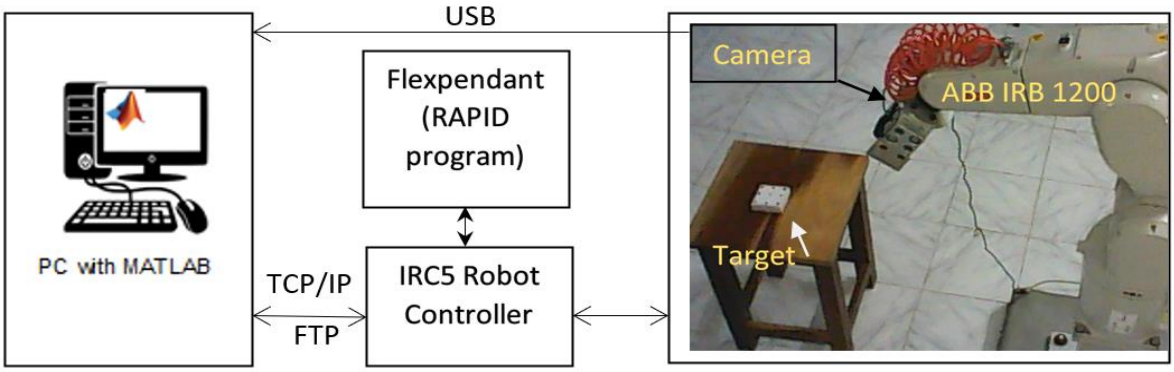

Figure 1 (a) Robot with end effector camera (b)

Figure 1 illustrates the comprehensive framework used to assess visual servoing on the ABB IRB 1200. The camera, mounted on the robot end effector, captures visual information. A MATLAB program processes this information to determine the target pose. Concurrently, MATLAB retrieves the robot's pose from the IRC5 robot controller using File Transfer Protocol (FTP). As the control law calculates the necessary movement, MATLAB transmits commands through the IRC5 and the FlexPendant. Figure 2 depicts the linear and angular components of the camera pose.

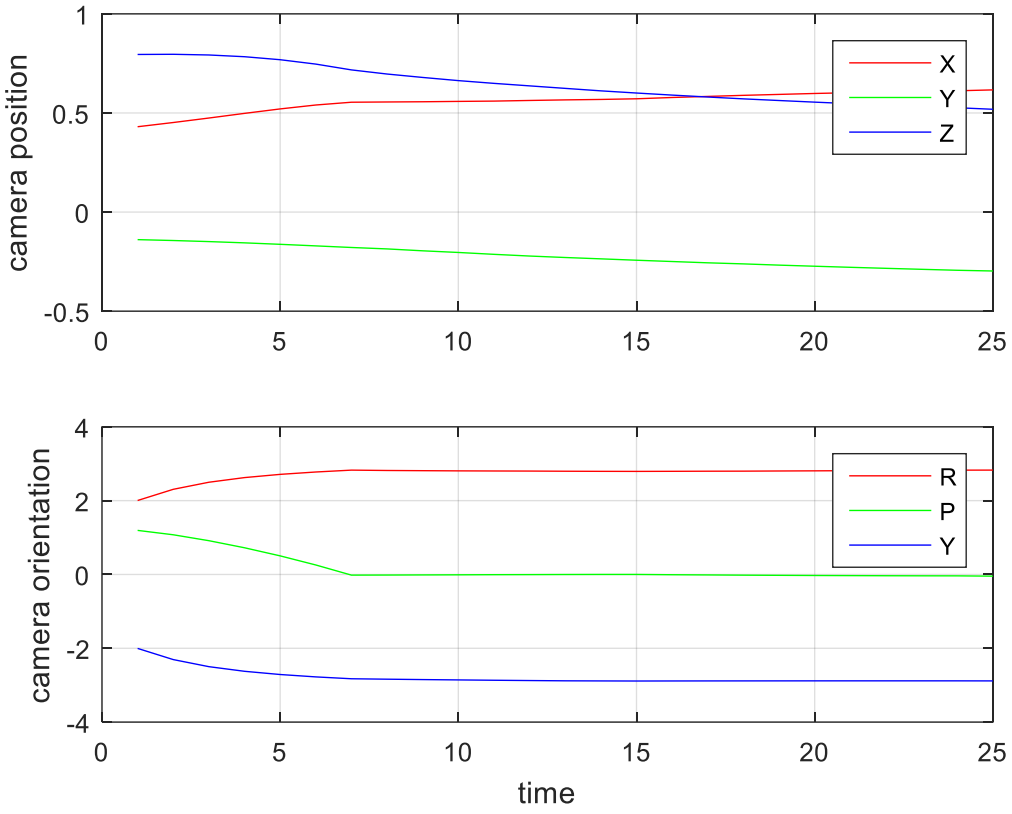

Figure 2 Variation of camera pose during servoing

Process Control Model

Typically, control problems are addressed in the context of single-loop systems where there is one manipulated variable and one controlled variable, referred to as Single Input Single Output (SISO) systems. However, practical problems in process control often involve more than one manipulated and controlled variable. These systems are categorized as Multiple Input Multiple Output (MIMO) systems (Figure 3). A distinctive feature of these control systems is the potential for interaction among different variables.

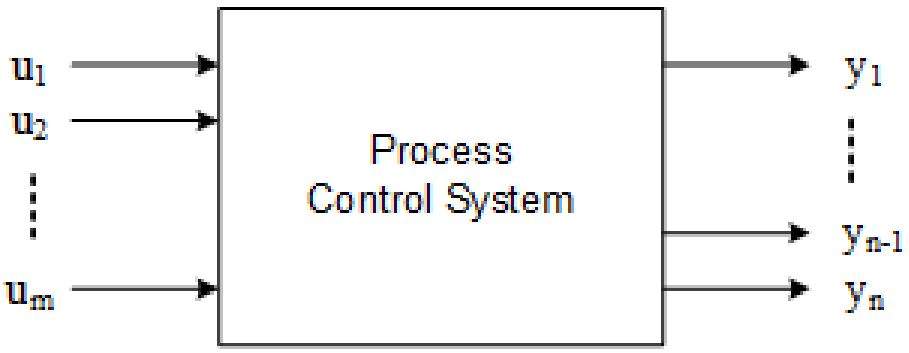

Figure 3 MIMO Control System

The control problem is a function of the system matrix $G(s)$ which is responsible for modifying the input vector $U(s)$ to derive the output variables $Y(s)$ (all the functions are written with Laplace operator) where

$Y(s) = G(s)U(s)$, (9)

$;U(s) = [u_1(s)\ \ u_2(s) \ldots\ldots u_m(s)\ ]^T$ and $Y(s) = [y_1(s)\ \ y_2(s) \ldots\ldots y_n(s)\ ]^T$

The multiplicity of variables gives rise to the chances of intertwined feedback loops. Each loop is prone to affect each other. This section will model the visual servo system as an MIMO system. As the camera moves, the way it sees the image features changes. This time variation from (6) is

$$\begin{bmatrix}\dot{x}\\ \dot{y}\end{bmatrix}=\begin{pmatrix}-\frac{1}{z} & 0 & \frac{x}{z} & xy & -(1+x^2) & y\\ 0 & -\frac{1}{z} & \frac{y}{z} & 1+y^2 & -xy & -x\end{pmatrix}\begin{bmatrix}\vartheta_x\\ \vartheta_y\\ \vartheta_z\\ \omega_x\\ \omega_y\\ \omega_z\end{bmatrix} \quad (10)$$

$$\begin{bmatrix}\dot{x}\\ \dot{y}\end{bmatrix}=[J_t]\begin{bmatrix}\vartheta_x\\ \vartheta_y\\ \vartheta_z\end{bmatrix}+[J_\omega]\begin{bmatrix}\omega_x\\ \omega_y\\ \omega_z\end{bmatrix} \quad (11)$$

J_t and J_ω are the interaction matrices for the linear and angular components and (10) and (11) show that the visual servo system has a MIMO structure (Vijayan and Ashok, 2017). Hence, there exists the possibility of decoupled-variable control in visual feedback systems.

Performance Analysis

When comparing the performance of Position-Based Visual Servoing (PBVS) and Image-Based Visual Servoing (IBVS), the latter is relatively robust and exhibits local asymptotic stability. However, IBVS is not without its drawbacks. The 2D information collected from the camera requires additional depth information for further processing. Given that the image controller has absolute control, uncertainties can lead to unnecessary camera motion. For instance, camera retreat might result in backward movement during pure rotational motion, causing features to converge linearly. There is a potential for encountering local minima in the trajectory and singularities in the interaction matrix when dealing with specific targets. In the upcoming session, the image-based controller in visual servoing will be modelled as a Multiple Input Multiple Output (MIMO) system. The characteristics of a feature change with even a slight adjustment in the camera's pose, which is reflected in the norm of the image Jacobian. Conversely, the norm of the inverse matrix signifies the variation in camera pose per unit change in the feature.

The norm of the inverse can undergo significant alterations for modest changes, even if the norm of the matrix remains relatively unchanged due to the ratio's multiplier effect. Another challenge arises from the linear dependence of vectors spanning the space. When the determinant of a matrix is zero, it signifies a subspace region within its appropriate space. If both translational and rotational elements share this subspace, it can lead to failure in servoing. The range space is critical in servoing, as velocity screws corresponding to motions outside this region can induce local minima with higher singular values in the system. To address these issues, specialized strategies such as decoupling, partitioning, and switching controls in visual servoing intentionally avoid the non-linearity of specific regions and the interaction of variables. Singular Value Analysis (SVA) and Relative Gain Array (RGA) can uncover the interaction within a multivariable system.

Manipulability of robots refers to its ease of obtaining arbitrary velocity in all directions and is expressed as the spherical nature of the ellipsoid represented by J*JT where J is the end effector Jacobian matrix. The radii of this ellipsoid represent the square roots of the Eigenvalues. The same approach to the visual servo model by considering a unit spatial velocity for the camera for the image Jacobian gives

$v_c{}^T v_c = 1,$

$\dot{p}^T {J_p}^{+T} {J_p}^{+} \dot{p} = 1,$

$$\dot{p}^T (J_p {J_p}^T)^{-1} \dot{p} = 1$$

The plots of ellipsoids represented by J*JT of the linear and angular blocks of the image Jacobian matrix show the manipulability of the robot with visual servo. The radii represent the singular values of the system, and the closeness of the shape to being spherical determines the wellness of the system.

Singular Value Analysis

The non-negative square roots of the eigenvalues of the product of a matrix and its transpose provide its singular values. The Condition Number (CN) is defined as the ratio of the largest and least nonzero singular values. CN serves as a subjective metric of performance, expressing the overall health of the system. A low CN value indicates a well-conditioned system, while a high value suggests the opposite. CN, as the product of the norms of the system matrix and its inverse, illustrates the ease of inverting the system. For a solution to the system of equations, the matrix must be non-singular. The wellness of the system is influenced by variable interaction. If the lowest singular value is close to the origin, indicating high interaction, the CN will be large. The third and sixth columns of the interaction matrix contain the optical axis components of linear and angular terms. Potential coupling between these columns can result in the camera moving backward. Selecting collinear points along the optical axis may trigger Jacobian singularities.

Relative Gain Array

Consider a MIMO system in open loop composition having p variables in the input 'u' and q variables in the output 'y'. A change in rth input , $\Delta \boldsymbol{r}$ with others remaining constant, affects the output of the system as $[\Delta \mathbf{1}, \Delta \mathbf{2}, \ldots \ldots \Delta \boldsymbol{yq}]$. The steady-state gain is given by $\boldsymbol{k_{jr}} = \frac{\Delta_{yj}}{\Delta_{ur}}$ where $\Delta_{\boldsymbol{yk}} = \mathbf{0} \quad \forall \boldsymbol{k} \neq \boldsymbol{j}$. When all the loops are closed except $\boldsymbol{ur} - \boldsymbol{yj}$ pair, the steady state gain in this case would be $\boldsymbol{l_{jr}} = \frac{\Delta_{yj}}{\Delta_{ur}}$; $\Delta_{\boldsymbol{yk}} = \mathbf{0} \quad \forall \boldsymbol{k} \neq \boldsymbol{j}$. If an interaction exists in $\boldsymbol{ur} - \boldsymbol{yj}$ pair, then $\boldsymbol{\lambda_{jr}} = \frac{\boldsymbol{k_{jr}}}{\boldsymbol{l_{jr}}}$ is called the relative gain. For any non-singular matrix $\boldsymbol{A}$ the matrix defining the RGA is

$$\boldsymbol{RGA}(\boldsymbol{A}) = \wedge(\boldsymbol{A}) = \boldsymbol{A} \otimes (\boldsymbol{A^{-1}})^{\boldsymbol{T}}. \qquad (13)$$

Here, $\otimes$ denotes the element-by-element multiplication represented by Hadamard product. The relative array sums up to unity both column-wise and row-wise. This allows the evaluation of input-output variable relations. Both the system matrix and its RGA have the same permutations along its rows and columns.

The chosen image points within the feature strive to follow a straight-line trajectory from their initial to the desired position as the control law aims to exponentially reduce the error. The third and sixth columns of the image Jacobian pertain to the z-axis and are frequently susceptible to interaction with certain feature choices. Consequently, in such cases, the row sum is less than one, leading to challenges in controlling the associated output. If one or more inputs have no impact on the output, the column sum in the Relative Gain Array (RGA) matrix will be less than one.

3. NUMERICAL ANALYSIS AND RESULTS

The subsequent sections address a scenario where the camera is positioned two meters away from the origin along the z-axis (0,0,2), while the target location is at the origin. In the image plane, a rectangular box placed at the origin will appear as a rectangle. Figure 4(a) depicts the camera views of the target at the beginning and end of the servoing process. Figure 4(b) shows the image plane variation during servoing. The forthcoming sections analyze the interaction matrix using Singular Value Analysis (SVA) and Relative Gain Array (RGA) for various camera locations. The final pose of the camera will be 0.25 meters in front of the target along the z-axis, and the error norm for this position is 0.5.

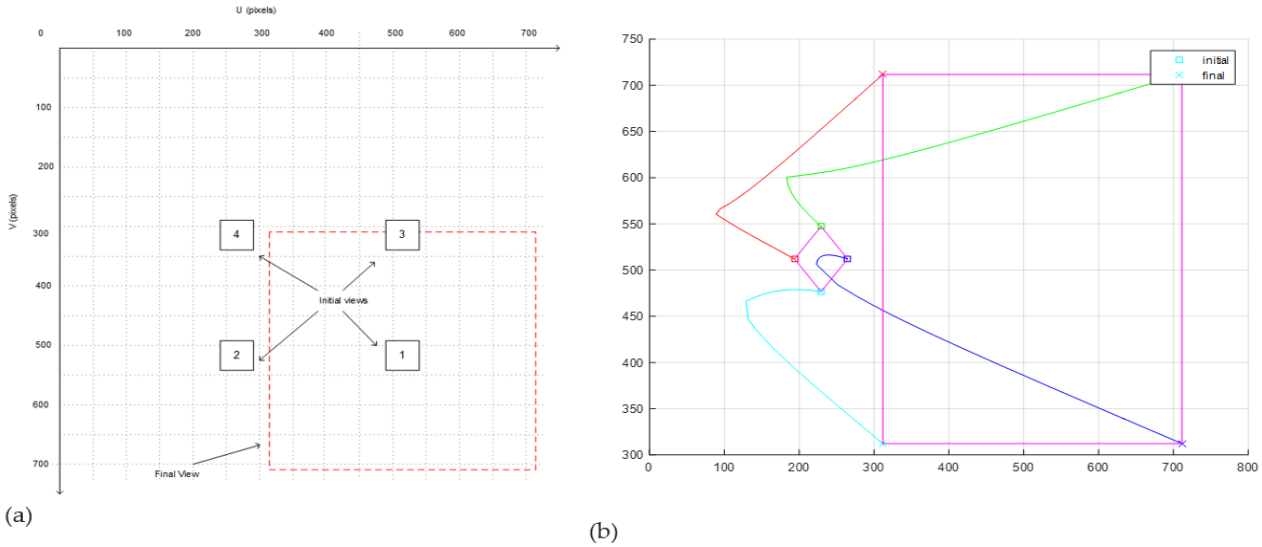

(a) (b)

Figure 4 (a) Initial and final feature points (b) Camera view during visual servoing

Translation along z-axis

Considering the initial pose of the camera, its movement is constrained solely along the z-axis. The image features considered are the four corners of the rectangle. The image plane coordinates for these corners are [(487, 487), (487, 537), (537, 537), (537, 487)] (Figure 4(a) object 1). As the final pose of the camera is predetermined, its pixel values are [(312, 312), (312, 712), (712, 712), (712, 312)]. The resulting interaction matrix has a 6x8 structure, originating from the selection of these four image features. The interaction matrix is computed using equation (6). From SVA, the singular values (S) and condition number CN are S = [452.84 452.84 70.71 35.35 2.76 2.76], $CN = \frac{452.84}{2.76} = 164.06$

The RGA matrix is given below.

$$\begin{bmatrix} 0.25 & 0 & 0.125 & 0.25 & 0 & 0.125 \\ 0 & 0.25 & 0.125 & 0 & 0.25 & 0.125 \\ 0.25 & 0 & 0.125 & 0.25 & 0 & 0.125 \\ 0 & 0.25 & 0.125 & 0 & 0.25 & 0.125 \\ 0.25 & 0 & 0.125 & 0.25 & 0 & 0.125 \\ 0 & 0.25 & 0.125 & 0 & 0.25 & 0.125 \\ 0.25 & 0 & 0.125 & 0.25 & 0 & 0.125 \\ 0 & 0.25 & 0.125 & 0 & 0.25 & 0.125 \end{bmatrix}$$

The Relative Gain Array (RGA) illustrates the characteristics of a matrix in good condition based on its element values. The RGA remains unchanged even when the depth is set at 4 meters. The singular values are given by S = [413.82, 413.82, 35.35, 8.83, 0.37, 0.37], resulting in a Condition Number (CN) of 1096. In terms of the condition number value, the matrix is not considered well-conditioned. However, the depth does not affect the controllability feature of visual feedback. As the camera attains the desired pose, the RGA remains constant, indicating good condition with a low value for the condition number. Figure 5 displays the velocity ellipsoids obtained for translation along the Z-axis alone.

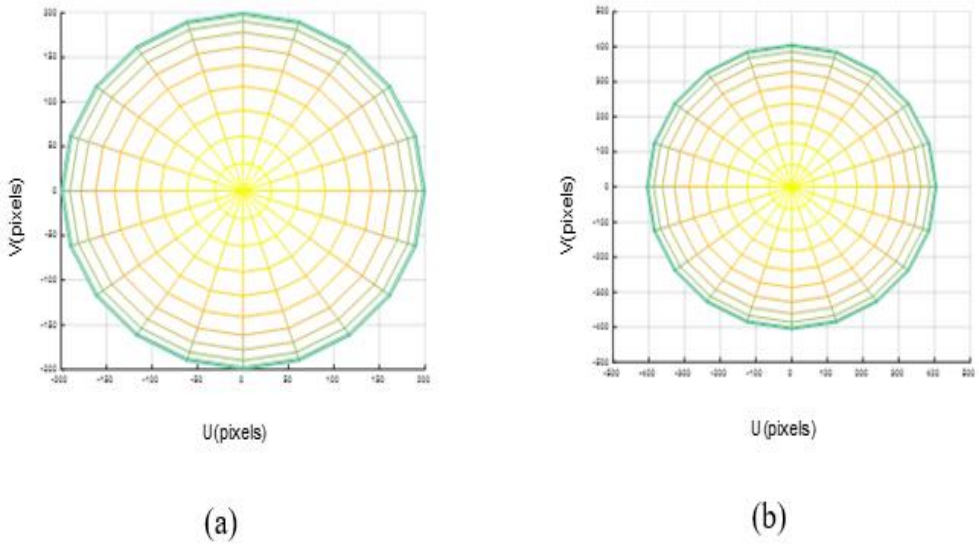

Figure 5 (a) Translational and (b) rotational velocity ellipsoids

Translation along z-axis

A translation of 2 meters along the x-axis affects the visibility of the target for the camera. Consequently, a translation of 2 meters is performed along both the x and z-axes. The updated coordinates of the target are [(287, 487), (287, 537), (337, 537), (337, 487)] (Figure 4(a) object 2). From the Singular Value Analysis (SVA) of the image Jacobian, the singular values are given by S = [861.9412, 605.1088, 79.4345, 27.8071, 10.5923, 10.5635], resulting in a Condition Number (CN) of 81.596.

$$\begin{bmatrix} -1.75 & 0 & -2.1477 & 0.3409 & 4.3939 & -0.0265 \\ 0 & -3.6894 & 0.3977 & 1.9697 & -0.2045 & 2.2159 \\ -1.75 & 0 & -2.1477 & 0.3409 & 4.3939 & -0.0265 \\ 0 & -3.6894 & 0.3977 & 1.9697 & -0.2045 & 2.2159 \\ 2.25 & 0 & 1.6705 & 0.1591 & -3.4242 & 0.0341 \\ 0 & 4.1894 & 0.5795 & -1.9697 & -0.2652 & -1.7235 \\ 2.25 & 0 & 1.6705 & 0.1591 & -3.4242 & 0.0341 \\ 0 & 4.1894 & 0.5795 & -1.9697 & -0.2652 & -1.7235 \end{bmatrix}$$

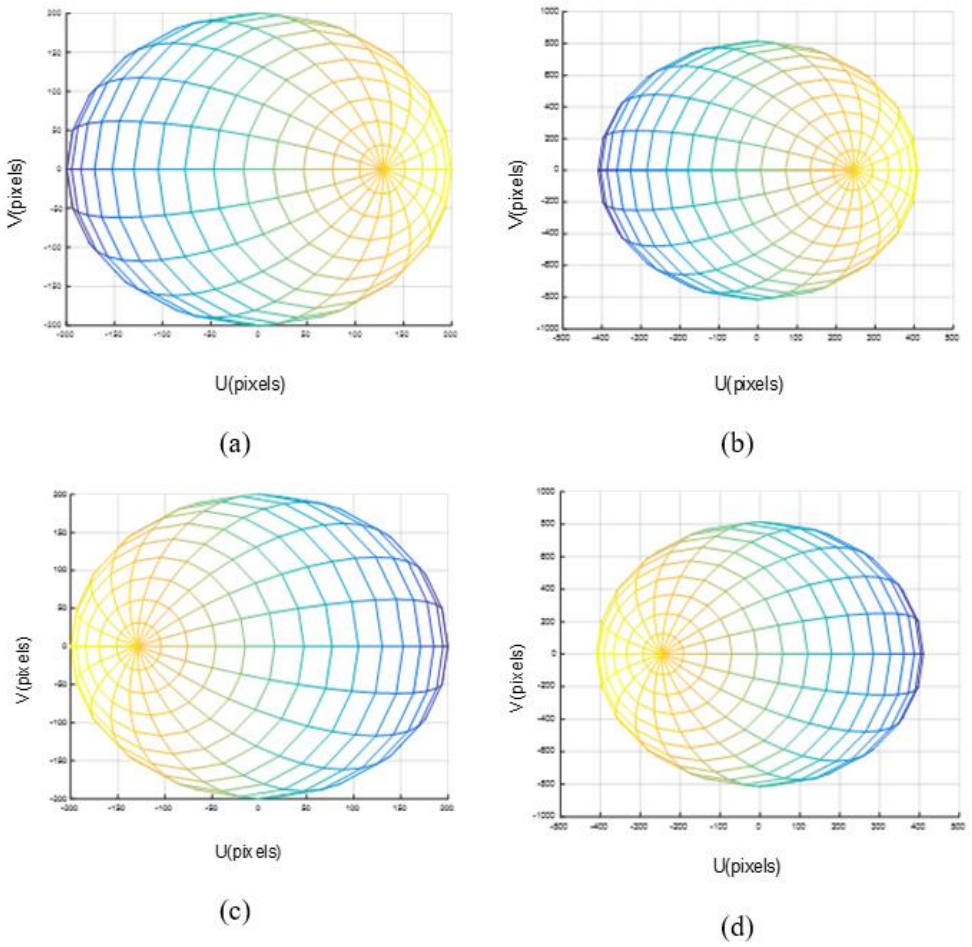

Figure 6 (a) Translational (a, c) and rotational (b, d) velocity ellipsoids for X-axis translation along positive and negative directions

Although the condition number is lower in comparison with the previous case, the elements of the Relative Gain Array (RGA), as provided above, are perturbed, indicating varied movements are required to modify each matrix element to achieve the final value. It is evident that the components of the first row, corresponding to the 'x' value of the coordinates, must undergo translation along the x and z-axes and rotation along the y-axis. When considering a translation of -2 meters along the x-axis, the Condition Number (CN) and singular values remain unchanged, but the RGA has altered due to the feature points being now located at [(687, 487), (687, 537), (737, 537), (737, 487)]. The elements of the RGA have interchanged their positions, indicating a symmetrical movement similar to the previous one. Figure 6 illustrates the translational and rotational velocity ellipsoids for translation along the X-axis in both positive and negative directions.

$$\begin{bmatrix} 2.25 & 0 & 1.6705 & 0.1591 & -3.4242 & 0.0341 \\ 0 & 4.1894 & 0.5795 & -1.9697 & -0.2652 & -1.7235 \\ 2.25 & 0 & 1.6705 & 0.1591 & -3.4242 & 0.0341 \\ 0 & 4.1894 & 0.5795 & -1.9697 & -0.2652 & -1.7235 \\ -1.75 & 0 & -2.1477 & 0.3409 & 4.3939 & -0.0265 \\ 0 & -3.6894 & 0.3977 & 1.9697 & -0.2045 & 2.2159 \\ -1.75 & 0 & -2.1477 & 0.3409 & 4.3939 & -0.0265 \\ 0 & -3.6894 & 0.3977 & 1.9697 & -0.2045 & 2.2159 \end{bmatrix}$$

Translation *along y-axis*

For a translation of 2 meters along the y-axis, the coordinates of the image corners are [(487, 287), (487, 337), (537, 337), (537, 287)] (Figure 4(a) object 3). According to the Singular Value Analysis (SVA), S = [861.94, 605.10, 79.43, 27.80, 10.59, 10.56], the Condition

Number is 81.59. The condition number and the singular values remain the same as for the translation along the X-axis. The Relative Gain Array (RGA) is provided in (Table 4). This matrix is similar to that of the translation along the X-axis, with the difference being the movement of the y-point of the feature in the former follows the x-point of the latter. Figure 7 illustrates the velocity ellipsoids corresponding to translational and rotational components. These results closely resemble those in Figure 6, differing only in the direction of the ellipse.

$$\begin{bmatrix} -3.6894 & 0 & 0.3977 & -0.2045 & 1.9697 & 2.2159 \\ 0 & -1.75 & -2.1477 & 4.3939 & 0.3409 & -0.0265 \\ 4.1894 & 0 & 0.5795 & -0.2652 & -1.9697 & -1.7235 \\ 0 & 2.25 & 1.6705 & -3.4242 & 0.1591 & 0.0341 \\ 4.1894 & 0 & 0.5795 & -0.2652 & -1.9697 & -1.7235 \\ 0 & 2.25 & 1.6705 & -3.4242 & 0.1591 & 0.0341 \\ -3.6894 & 0 & 0.3977 & -0.2045 & 1.9697 & 2.2159 \\ 0 & -1.75 & -2.1477 & 4.3939 & 0.3409 & -0.0265 \end{bmatrix}.$$

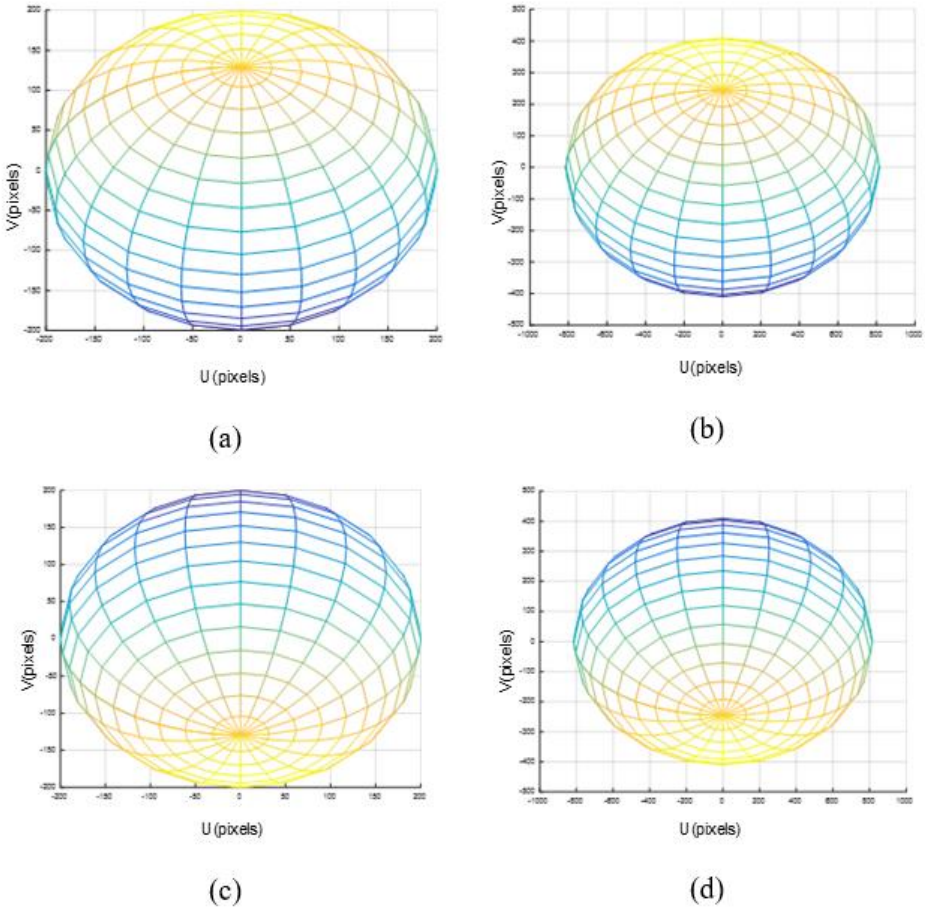

Figure 7 Translational (a, c) and rotational (b, d) velocity ellipsoids for Y-axis translation along positive and negative directions

Translation along X, Y, and Z axes

Considering a translation along all the axes by 2 meters, the pixel coordinates of the target are given by [(287, 287), (287, 337), (337, 337), (337, 287)] (Figure 4(a) object 4). The singular values are S = [1265.12, 725.65, 91.57, 25.82, 10.90, 10.72], and the Condition Number (CN) is 117.97. Despite the favorable condition number, the singular values have high magnitudes due to both the highest and lowest singular values being large. The Relative Gain Array (RGA) is provided below. The deviation from the nominal values of the RGA matrix, as represented in the first case, indicates the target is positioned away from the camera. Figure 8 illustrates the velocity ellipsoids for translational and rotational motion.

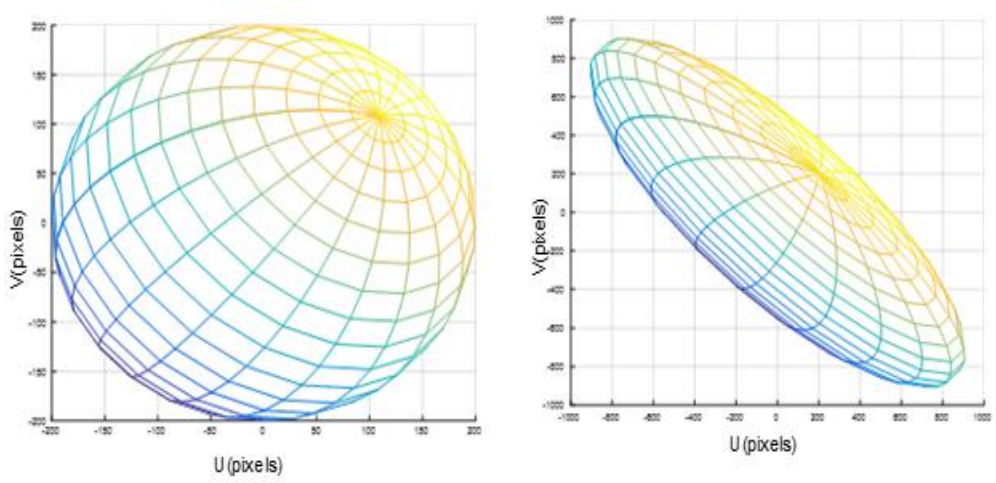

Figure 8 Translational and rotational velocity ellipsoids for translation along X, Y and Z axes

Now, let us consider a rotation along the Cartesian axes. A nominal value of 0.1 radians is chosen to observe the effect of rotation on the RGA.

$$\begin{bmatrix} -3.5038 & 0 & -2.6135 & 0.3115 & 4.4615 & 2.0942 \\ 0 & -3.5038 & -2.6135 & 4.4615 & 0.3115 & 2.0942 \\ -1.9654 & 0 & 4.8635 & -2.1808 & 0.000 & 0.0942 \\ 0 & 1.9731 & -3.1365 & 0.000 & 1.6962 & 0.1558 \\ 4.4962 & 0 & 1.3865 & 0.1885 & -3.4769 & -1.8442 \\ 0 & 4.4962 & 1.3865 & -3.4769 & 0.1885 & -1.8442 \\ 1.9731 & 0 & -3.1365 & 1.6962 & -0.000 & 0.1558 \\ 0 & -1.9654 & 4.8635 & -0.000 & -2.1808 & 0.0942 \end{bmatrix}$$

Rotation along X-axis

The camera is rotated from its initial pose by an angle of 0.1 radians along the x-axis, and the new coordinates of the target are [(487.18, 507.13), (486.55, 557.63), (537.44, 557.64), (536.81, 507.13)]. The singular values are given by S = [457.305, 454.7624, 71.2813, 35.4708, 3.2643, 3.1872], and the Condition Number (CN) is 143.48. The Relative Gain Array (RGA) is provided below. The linear velocity along the x-axis and angular velocity along the y-axis of the x-coordinate are affected. For the y-coordinate, it is the linear velocity along the y-axis and angular velocity along the x-axis that are affected.

$$\begin{bmatrix} 5.3883 & 0 & 0.4453 & 0.0510 & -5.0095 & 0.0303 \\ 0 & 5.1158 & 0.0065 & -4.7174 & 0.0204 & 0.1638 \\ -4.8883 & 0 & -0.0123 & 0.2063 & 5.0134 & 0.2841 \\ 0 & -4.6158 & 0.0606 & 4.9601 & 0.4757 & 0.0218 \\ -4.8883 & 0 & -0.0123 & 0.2063 & 5.0134 & 0.2841 \\ 0 & -4.6158 & 0.0606 & 4.9601 & 0.4757 & 0.0218 \\ 5.3883 & 0 & 0.4453 & 0.0510 & -5.0095 & 0.0303 \\ 0 & 5.1158 & 0.0065 & -4.7174 & 0.0204 & 0.1638 \end{bmatrix}$$

Rotation along the Y-axis

For a camera rotation of 0.1 radians along the y-axis, the interpretations are similar to that of the rotation along the x-axis. The target features are located at [(466.36, 486.55), (466.36, 537.44), (516.87, 536.81), (516.87, 487.18)]. The singular values are given by S=[457.305,454.7624,71.2813,35.4708,3.2643,3.1872], and the Condition Number (CN) is 143.48. These values are the same as those

obtained with rotation along the x-axis. The Relative Gain Array (RGA) values are provided in the following matrix. The direction of the action of variables has changed. The linear velocity along the x-axis and angular velocity along the y-axis of the x-coordinate are affected. For the y-coordinate, it is the linear velocity along the y-axis and angular velocity along the x-axis that are affected.

$$\begin{bmatrix} -4.6158 & 0 & 0.0606 & 0.4757 & 4.9601 & 0.0218 \\ 0 & -4.8883 & -0.0123 & 5.0134 & 0.2063 & 0.2841 \\ -4.6158 & 0 & 0.0606 & 0.4757 & 4.9601 & 0.0218 \\ 0 & -4.8883 & -0.0123 & 5.0134 & 0.2063 & 0.2841 \\ 5.1158 & 0 & 0.0065 & 0.0204 & -4.7174 & 0.1638 \\ 0 & 5.3883 & 0.4453 & -5.0095 & 0.0510 & 0.0303 \\ 5.1158 & 0 & 0.0065 & 0.0204 & -4.7174 & 0.1638 \\ 0 & 5.3883 & 0.4453 & -5.0095 & 0.0510 & 0.0303 \end{bmatrix}$$

Rotation along the Z-axis

A rotation of the z-axis will alter the view of the camera. First, consider a rotation of 0.1 radians along the z-axis. The corresponding points in the image feature are [(484.62, 489.62), (489.62, 539.37), (539.37, 534.37), (534.37, 484.62)]. The singular values are S= [457.30,454.76,71.28,35.47,3.26,3.18], and the condition increases to 164.06. The Relative Gain Array (RGA) is as below:

$$\begin{bmatrix} -2.9784 & 0 & 0.1498 & 0.2401 & 3.2382 & 0.1002 \\ 0 & 3.4784 & 0.1002 & -3.2185 & 0.2401 & 0.1498 \\ 3.4784 & 0 & 0.1002 & 0.2401 & -3.2185 & 0.1498 \\ 0 & -2.9784 & 0.1498 & 3.2382 & 0.2401 & 0.1002 \\ -2.9784 & 0 & 0.1498 & 0.2401 & 3.2382 & 0.1002 \\ 0 & 3.4784 & 0.1002 & -3.2185 & 0.2401 & 0.1498 \\ 3.4784 & 0 & 0.1002 & 0.2401 & -3.2185 & 0.1498 \\ 0 & -2.9784 & 0.1498 & 3.2382 & 0.2401 & 0.1002 \end{bmatrix}$$

For a rotation by $\pi/6$ radians along the optical axis, the key points move to [(477.84,502.84), (502.84, 546.84), (546.15,521.15), (521.15,477.84)]. In SVA, condition number and the singular values do not change, but the RGA matrix shows severe perturbation in the (shown below) columns 1, 2, 4 and 5. However, the effect is negligible for rotation by $\pi/2$ or its multiples in the RGA. The translational and rotational velocity ellipsoids for rotation along the three axes by 0.1 radians is given in (Figure 9). Compared with translation the ellipsoids are very similar.

$$\begin{bmatrix} -13.8229 & 0 & 0.2333 & 0.0625 & 14.2604 & 0.0167 \\ 0 & 14.3229 & 0.0167 & -13.8854 & 0.0625 & 0.2333 \\ 14.3229 & 0 & 0.0167 & 0.0625 & -13.8854 & 0.2333 \\ 0 & -13.8229 & 0.2333 & 14.2604 & 0.0625 & 0.0167 \\ -13.8229 & 0 & 0.2333 & 0.0625 & 14.2604 & 0.0167 \\ 0 & 14.3229 & 0.0167 & -13.8854 & 0.0625 & 0.2333 \\ 14.3229 & 0 & 0.0167 & 0.0625 & -13.8854 & 0.2333 \\ 0 & -13.8229 & 0.2333 & 14.2604 & 0.0625 & 0.0167 \end{bmatrix}$$

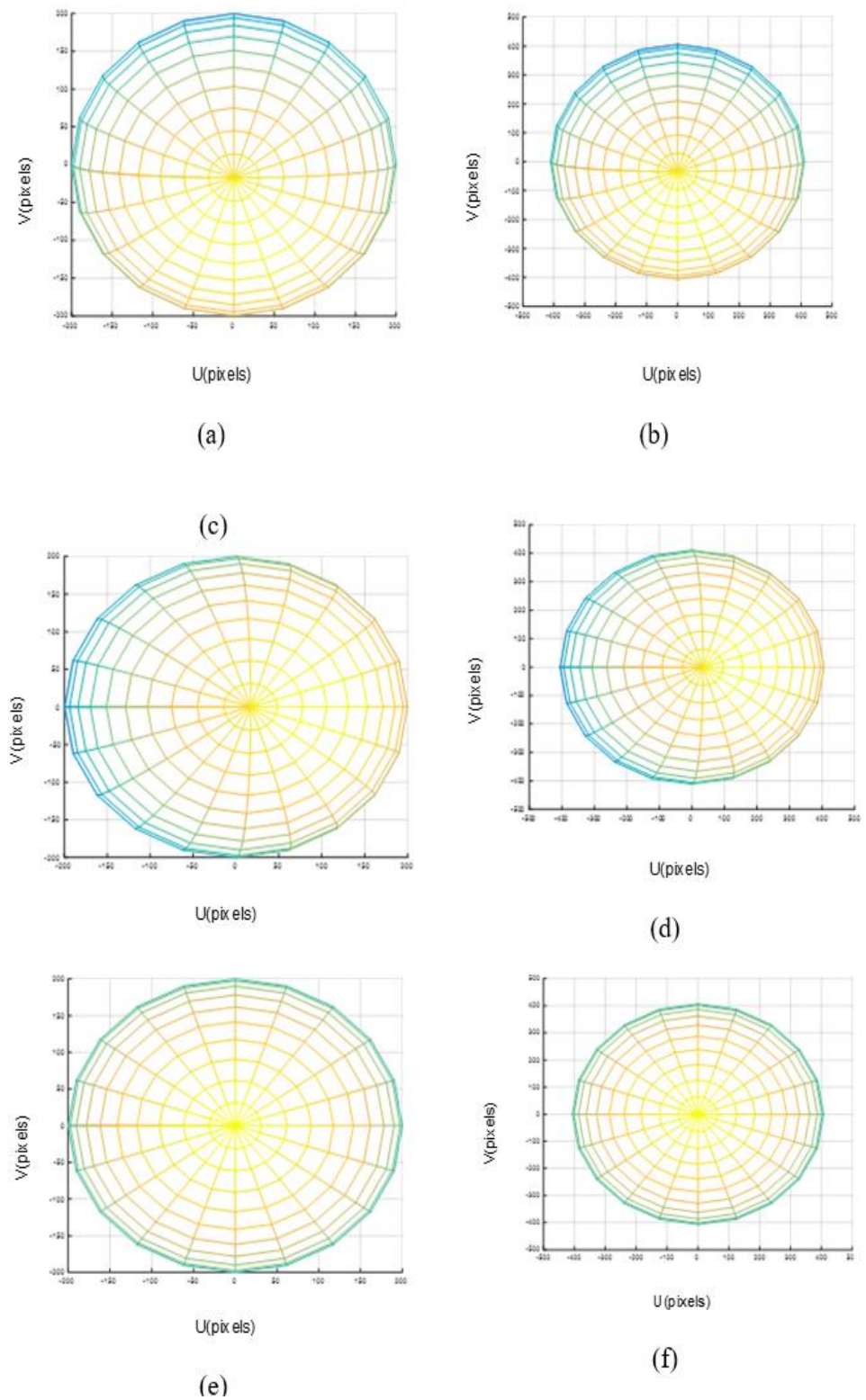

Figure 9 Velocity ellipsoids for translational (a, c, e) and rotational (b, d, f) motion for rotations along X, Y and Z axes

Singularities

As mentioned earlier, the selection of image points is crucial. Let's consider only three feature points along the y-axis of the pixel plane: [(487, 487), (512, 487), (537, 487)]. Singular Value Analysis (SVA) yields S=[392.92, 392.77, 35.6318, 17.5398, 1.1160, 0.0000]. Note that the last singular value is very close to zero, indicating a high Condition Number (CN) and an ill-conditioned system. The singular matrix provides no output for the control law, and the Relative Gain Array (RGA) is presented below:

$$\begin{bmatrix} -32.50 & 0 & 0.5 & 0.0000 & 32.5 & 0.5000 \\ 0 & 0.0699 & -0.0041 & 0.2674 & -0.0000 & 0.5000 \\ 66.0 & 0 & 0.0 & -0.000 & -64.00 & -1.000 \\ 0 & 0.0699 & -0.0041 & 0.2674 & 0.0000 & 0.0000 \\ -32.50 & 0 & 0.499 & 0.0000 & 32.500 & 0.5000 \\ 0 & 0.0699 & -0.0041 & 0.2674 & 0.0000 & 0.5000 \end{bmatrix}$$

As the rows and columns do not sum to unity, the control structure is ineffective. Consider changing the third point to (537, 486.5). The new singular values are S=[392.96, 392.84, 35.6379, 17.5391, 1.1272, 0.0113], indicating an invertible matrix with a very high Condition Number (CN) of 34660. The Relative Gain Array (RGA) is provided below:

$$\begin{bmatrix} -32.171 & 0 & 0.51494 & -0.00989 & 32.1718 & 0.4949 \\ 0 & -3200.12 & -50.5149 & 3250.64 & 0.50504 & 0.4949 \\ 65.98 & 0 & 0 & 0 & -63.9873 & -0.9998 \\ 0 & 6400.0 & 101.000 & -6500.00 & 0 & 0 \\ -32.8152 & 0 & 1.4947 & -1.0097 & 32.8152 & 0.5149 \\ 0 & -3198.87 & -51.4947 & 3251.376 & 0.5048 & 0.4949 \end{bmatrix}$$

Large elements present in the Relative Gain Array (RGA) indicate uncertainty in the operation due to the interaction of control variables. The lowest singular value being near zero indicates an ill-conditioned system. If the last point selected was (537.5, 487), the uncertainty would have been in the x-component of the output, which is also near singularity. Hence, an alternative is to add a fourth point as [(487, 487), (512, 487), (537, 487), (537, 537)]. The new set of singular values is S=[454.40, 450.94, 60.0103, 29.9158, 2.1801, 1.9670], and the Condition Number (CN) is 231.02. The RGA is as given below. The large RGA elements have less magnitude compared to the former approach.

$$\begin{bmatrix} -19.4581 & 0 & 0.2515 & 0.2665 & 19.6557 & 0.2485 \\ 0 & 14.9311 & 0.2066 & -14.7904 & 0.2305 & 0.2066 \\ 13.8323 & 0 & 0 & 0 & -13.4132 & 0.0060 \\ 0 & 5.3054 & 0.0838 & -5.0599 & 0 & 0 \\ -6.4162 & 0 & -0.0030 & 0.4671 & 6.8114 & -0.0030 \\ 0 & -4.3204 & -0.0389 & 4.6707 & 0.3623 & 0.0389 \\ 13.0419 & 0 & 0.2485 & 0.2665 & -12.8443 & 0.2515 \\ 0 & -14.9162 & -0.2515 & 15.1796 & 0.1976 & 0.2515 \end{bmatrix}$$

Consider three points along the vertical axis of the image plane: [(487, 487), (487, 512), (487, 537)]. The singular values are S = [392.92, 392.77, 35.6318, 17.5398, 1.1160, 0.0000] with a very high Condition Number. The Relative Gain Array (RGA) in this case is provided below. The difference from the three collinear points along the horizontal axis is the uncertainty in the x-element of the features:

$$\begin{bmatrix} 0.0700 & 0 & -0.0041 & -0.0000 & 0.2675 & 0.5000 \\ 0 & -32.500 & 0.5000 & 32.500 & 0.0000 & 0.5000 \\ 0.0700 & 0 & -0.0041 & 0 & 0.2675 & 0 \\ 0 & 66.000 & 0 & -64.000 & 0 & -1.000 \\ 0.0700 & 0 & -0.0041 & 0.0000 & 0.2675 & 0.5000 \\ 0 & -32.500 & 0.5000 & 32.5000 & -0.0000 & 0.5000 \end{bmatrix}$$

The suggested solution in this case is also the addition of a fourth point in the features so that the matrix can be inverted, rather than selecting a near-singular point. Also, consider three points along the x-y plane: [(487, 487), (512, 512), (537, 537)]. The new set of

singular values is S= [393.79, 387.29, 50.0000, 25.0000, 2.2445, 0.0000] with a very high Condition Number. The Relative Gain Array (RGA) in this case is shown below:

$$\begin{bmatrix} -7.9667 & 0 & 0.2500 & 0.1229 & 8.2604 & 0.2500 \\ 0 & -7.9667 & 0.2500 & 8.2604 & 0.1229 & 0.2500 \\ 16.5333 & 0 & 0 & 0 & -15.8667 & 0 \\ 0 & 16.5333 & 0 & -15.8667 & 0 & 0 \\ -7.9667 & 0 & 0.2500 & 0.1229 & 8.2604 & 0.2500 \\ 0 & -7.9667 & 0.2500 & 8.2604 & 0.1229 & 0.2500 \end{bmatrix}$$

It is clear that the selected variables are linearly dependent, indicating that one or more inputs do not have any effect on the output. The addition of a point in the grid is suggested to ensure an invertible matrix for visual servoing.

4. CONCLUSION

This paper aimed to develop a multivariable model for a visual servo system and evaluate its Relative Gain Array (RGA) for performance analysis. The RGA can indicate the sensitivity to uncertainty of its input channels and elements. If the elements of the RGA are large, inverse-based controllers are less useful, especially around their corner frequencies. Physical coupling between transfer function elements can lead to rare but significant element uncertainty. If local minima or singularity is associated with significant translational motion, servoing will fail. If an element of the interaction matrix changes from its previous value, equaling the inverse of the corresponding RGA component, matrix inversion becomes impossible. This will result in unpredictable camera trajectories.

The Relative Gain Array of the interaction matrix helps explain its condition while undergoing servoing from an initial pose. For example, for Z-axis translational motion, the RGA will remain the same for different depths, while the Condition Number increases with the distance along the Z-axis, as explained by the scaling property of RGA. A rotation by multiples of $\pi/2$ merely alters the position of the elements of the array, but CN does not change. For an RGA matrix with a full column rank, the column sum of its elements is unity. The ratio of columns and rows determines the sum of its row elements. One can choose to omit an input when the column sum falls below unity. Similarly, a row sum less than unity indicates difficulty in controlling the corresponding output.

Both the Condition Number and Relative Gain Array are crucial considerations for arriving at conclusions regarding the characteristics of the interaction matrix. When the maximum singular value is significantly higher than the minimum singular value, or the latter is extremely small compared to the former, the CN is high. A singular value being near zero is undesirable, as it indicates that the system is near singularity. For example, in visual servoing, three collinear points can induce a singular interaction matrix. Hence, the selection of image features is critical for the convergence of the control law.

Authors Contributions

Abhilash T, Vijayan completed his doctoral research in Robotics and automation with the title “visual servoing of a 6 DOF industrial robot” under the guidance of Dr. Ashok S, Professor, EE, NIT Calicut.

Ethical issues

Not applicable.

Informed consent

Not applicable.

Funding

This study has not received any external funding.

Conflict of Interest

The author declares that there are no conflicts of interests.

Data and materials availability

All data associated with this study are present in the paper.

REFERENCES AND NOTES

1. Bristol E. On a new measure of interaction for multivariable process control. IEEE Trans Aut Con 1966; 11(1):133-134.
2. Chaumette F, Hutchinson S. Visual servo control. I. Basic approaches. IEEE Rob Autom Mag 2006; 13(4):82-90.
3. Chen J, Freudenberg JS, Nett CN. The role of the condition number and the relative gain array in robustness analysis. Automatica 1994; 30(6):1029-1035.
4. Deguchi K. Optimal motion control for image-based visual servoing by decoupling translation and rotation. IEEE/RSJ Int Con on Intell Robots and Systems 1998; 705-711.
5. Gangloff JA, de-Mathelin MF. High speed visual servoing of a 6 DOF manipulator using MIMO predictive control. IEEE Int Con on Robot Autom 2000; 4:3751-3756.
6. Hutchinson S, Hager GD, Corke PI. A tutorial on visual servo control. IEEE Trans on Robot Autom 1996; 12(5):651-670. doi: 10.1109/70.538972
7. Merlet JP. Jacobian, Manipulability, Condition Number, and Accuracy of Parallel Robots. J Mech Des Trans ASME 2006; 128(1):199-206.
8. Seborg DE. Process Dynamics and Control. Fourth edition. Wiley 2011; 463.
9. Siebel NT, Peters D, Sommer G. Models and Control Strategies for Visual Servoing. In: Visual Servoing, Rong-Fong Fung (Ed.) 2010.
10. Vijayan A, Ashok S. A MIMO Approach to Supervisory Control in Robot Visual Feedback. IREMOS 2017; 10(1):16-25.